#### COMMUNICATION



# Early dynamic changes in iPSC oxygen consumption rate predict future cardiomyocyte differentiation

Arina A. Nikitina<sup>1</sup> | Tanya Roysam<sup>2</sup> | Melissa L. Kemp<sup>2,3</sup>

<sup>1</sup>School of Biological Sciences, Georgia Institute of Technology, Atlanta, Georgia, USA

<sup>2</sup>The Wallace H. Coulter Department of Biomedical Engineering, Georgia Institute of Technology and Emory University, Atlanta, Georgia, USA

<sup>3</sup>Petit Institute of Bioengineering and Biosciences, Georgia Institute of Technology, Atlanta, Georgia, USA

#### Correspondence

Melissa L. Kemp, The Wallace H. Coulter Department of Biomedical Engineering. Georgia Institute of Technology and Emory University, Atlanta, GA, USA. Email: melissa.kemp@bme.gatech.edu

**Funding information** National Science Foundation

## **Abstract**

Human induced pluripotent stem cells (iPSCs) hold great promise for reducing the mortality of cardiovascular disease by cellular replacement of infarcted cardiomyocytes (CMs). CM differentiation via iPSCs is a lengthy multiweek process and is highly subject to batch-to-batch variability, presenting challenges in current cell manufacturing contexts. Real-time, label-free control quality attributes (CQAs) are required to ensure efficient iPSC-derived CM manufacturing. In this work, we report that live oxygen consumption rate measurements are highly predictive CQAs of CM differentiation outcome as early as the first 72 h of the differentiation protocol with an accuracy of 93%. Oxygen probes are already incorporated in commercial bioreactors, thus methods presented in this work are easily translatable to the manufacturing setting. Detecting deviations in the CM differentiation trajectory early in the protocol will save time and money for both manufacturers and patients, bringing iPSC-derived CM one step closer to clinical use.

## KEYWORDS

cell manufacturing, critical quality attributes, induced pluripotent stem cells, machine learning, oxygen consumption rate, time-series analysis

## 1 | INTRODUCTION

Cardiovascular diseases account for more than 30% of all deaths worldwide (World Health Organization [WHO], 2021). Such a high mortality rate is explained by the death of cardiomyocytes (CMs), which provide mechanical contractile function in the heart and have low regeneration ability postinfarction (van Berlo & Molkentin, 2014). Human induced pluripotent stem cells (iPSCs) are emerging as a promising tool for the replacement of the lost CM population (Guan et al., 2020; Shiba et al., 2016); however, differentiation of iPSCs into mature CMs is a lengthy process with many critical parameters influencing yields, resulting in a heterogeneity of outcomes (Floy et al., 2022). Poor predictability of the CM differentiation outcome will inevitably contribute to the already high cell manufacturing costs (Vormittag et al., 2018) and hinder the industrial scaling of iPS cell-based therapies for cardiac diseases. Developing a noninvasive label-free differentiation

success prediction method can prevent wasting time and reagent resources on a batch bound to fail.

Several recent studies have made advances towards the goal of CM differentiation batch prediction by label-free methodologies. The first study used live two-photon microscopy in 2D iPSC cultures to predict the CM differentiation outcome as early as day 1 using autofluorescence intensity of such metabolites FAD and NAD(P)H in a multivariate classification model (Qian et al., 2021). A different study measured various process parameters during CM differentiation in stir-tank bioreactors, including dissolved oxygen concentration in the media, to predict a failed batch by day 7 with an accuracy of 90% using multifactorial process modeling (Williams et al., 2020). Both approaches relied upon manually collecting samples from the bioreactor and/or specialized microscopy, which in a manufacturing setting increases the process complexity and workforce skill requirements. Here we present a prognostic model for CM differentiation outcome in the commonly studied WTC11 human

2357

10970290, 2023, 8, Downloaded from https://analytica

com/doi/10.1002/bit.28489 by Georgia

Institute Of Technology, Wiley Online Library on [11/07/2024]. See the Terms

on Wiley Online Library for rules of use; OA

articles are governed by the applicable Creative Comm

**FIGURE 1** Schematic of the experimental setup for oxygen consumption rate measurement during cardiomyocyte differentiation. CM differentiation was performed based upon Lian et al. (2012) with media changes reflected in discontinuities of OCR trajectories. OCR, oxygen consumption rate.

iPS cell line that requires only an oxygen consumption rate (OCR) measurement for the first 72 hours of a differentiation protocol for predicting cTnT expression on day 16. Dissolved oxygen concentration measurement is easily incorporated in commercial stir-tank bioreactors (Manstein et al., 2021; Williams et al., 2020), therefore, translation of an OCR-based prognosis model to an in-line, closed system manufacturing setting should come naturally.

### 2 | RESULTS AND DISCUSSION

CM differentiation was conducted in 96-well plates, in the 32 wells matching the oxygen probe locations of the RESIPHER plate lids (Lucid Scientific). A schematic of the experiment setup is shown in Figure 1. Each well produced a continuous read-out of the total oxygen consumption in the well; the reads were automatically taken every 15 min during the first 6 days of the CM differentiation (days 0-5 of the protocol), resulting in a total of 576 oxygen consumption measurements per well. A total of 10 experiments were conducted with seeding densities in the range of  $1-3.5 \times 10^4$  cells and CHIR99021 concentrations in the range of 3-14 µM, resulting in a dataset of 320 individual time series (Figure 2a). The deviation from the parameters in the standard differentiation protocol was introduced to produce a variety of CM yields for training a machine learning model. CM yield was measured on day 16 of the protocol by staining cells for cardiac troponin T (cTnT). The wells were split into six groups based on the resulting cTnT content: high cTnT (60%-90% cTnT positive signal in a well), 30%-60%, 15%-30%, 10%-15%, low but positive cTnT (<10%) and no cTnT (<1%). Our results indicate that on average lower oxygen consumption during the first 6 days of the CM differentiation protocol results in higher cTnT-positive signal (Figure 2b). The decrease in mitochondrial content has been reported during mesoderm differentiation (Mostafavi et al., 2021) which our findings may capture and attribute to the subsequent successful CM differentiation.

However, as shown in Figure 2b, the standard deviation of the oxygen consumption for each cTnT class is high, resulting in a significant overlap between classes. These considerations lead to the creation of the 174 time-series feature set which includes median

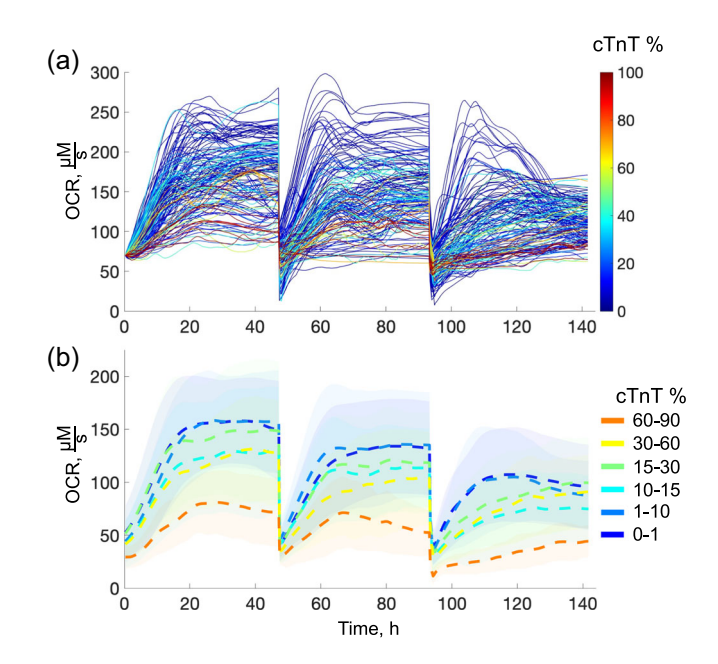


**FIGURE 2** Dynamic oxygen consumption changes during cardiomyocyte differentiation. (a) All time-series from 10 experiments, colored by the end-point cTnT expression measurement. The time series were translated to start from the same level of flux for clarity. (b) Time series split into six groups based on the end-point cTnT expression measurement, with dashed line representing the mean value and the shaded area representing the standard deviation.

oxygen consumption levels at various time windows, curve shape metrics (such as minimum and maximum values, times when those values are reached, etc.) and the same set of metrics for the derivative of the time series. In addition, 22 canonical time-series characteristics (catch22 [Lubba et al., 2019]) were added as extra time-series features. To test the predictive power of oxygen consumption data from the first 6 days of the CM differentiation and to validate the time series metrics we derived from those data we performed a partial least-squares regression (PLSR) against the endpoint cTnT expression. PLSR yielded a validation  $R^2$  of 0.83, revealing time series features that are highly predictive of cTnT expression (Figure 3).



0970290, 2023, 8, Downloaded

Institute Of Technology, Wiley Online Library on [11/07/2024]. See the Term

by the applicable

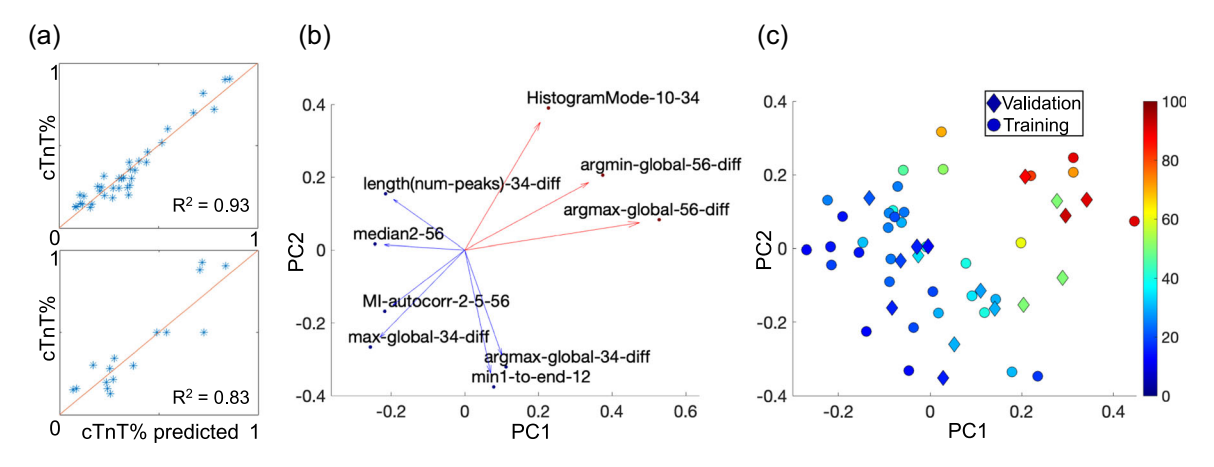


FIGURE 3 Partial least-squares regression (PLSR) with time series features against the end-point cTnT expression. (a) Regression prediction for the training ( $R^2 = 0.93$ ) and validation dataset ( $R^2 = 0.83$ ). A total of three principal components were used for cTnT prediction. (b) PLSR loadings plot featuring variables with variables of importance (VIP) > 1. Vectors are colored according to their regression coefficient value, with positive regression coefficients colored red and negative colored blue. (c) PLSR scores plot showing separation of wells with high and low cTnT. Data points are colored according to the cTnT expression. Yvar = 59%, 29%, and 5% for PC1, PC2, and PC3 accordingly.

The features represented in Figure 3b are the result of a sequential variable trimming with a 100-fold cross-validation accuracies compared with and without a given variable; only the features that reduce the R<sup>2</sup> value of the regression when removed from the dataset were retained. The goal of this method, however, is not in predicting continuous values of cTnT signal, but rather predicting a binary outcome of the protocol (success vs. failure). Thus, to split the data into cTnT positive and cTnT negative classes we used histogram-based thresholding of the cTnT expression values in our dataset, which vielded a threshold of 30%. After thresholding, only 27 time-series were retained as a cTnT positive class. An example of using a higher threshold (70%) is shown in Figure \$1, and with only 7 cTnT positive data points the model still performs well. However, to draw reliable conclusions in this article we demonstrate outcomes with a threshold of 30%. To perform a balanced PLS discriminant analysis (PLS-DA) with such limited data, for every cross-validation round a random sample of 27 cTnTsamples was selected to complement the existing 27 cTnT+ samples. After a sequential variable trimming with a 100-fold cross-validation performed in the same manner as it was for PLSR, the PLS-DA model yielded 93% validation accuracy. We calculated how validation accuracy changed with length of the time series used for prediction and observed that it stopped growing after first 72 h of the data was included (Figure 4b). The discriminant model results in clear class separation as shown in the biplot (Figure 4a) with the retained time series metrics. Our analysis suggest that manufacturers can conclude whether the CM differentiation is going to succeed after only 72 hours after the protocol was initiated with an accuracy of 93%. To check if our model was affected by changes in cell count during CM differentiation due to cell death or changes proliferation speed, we used a WTC11 lamin-B1 GFP reporter cell line to normalize the OCR by cell count. Our results do not indicate an

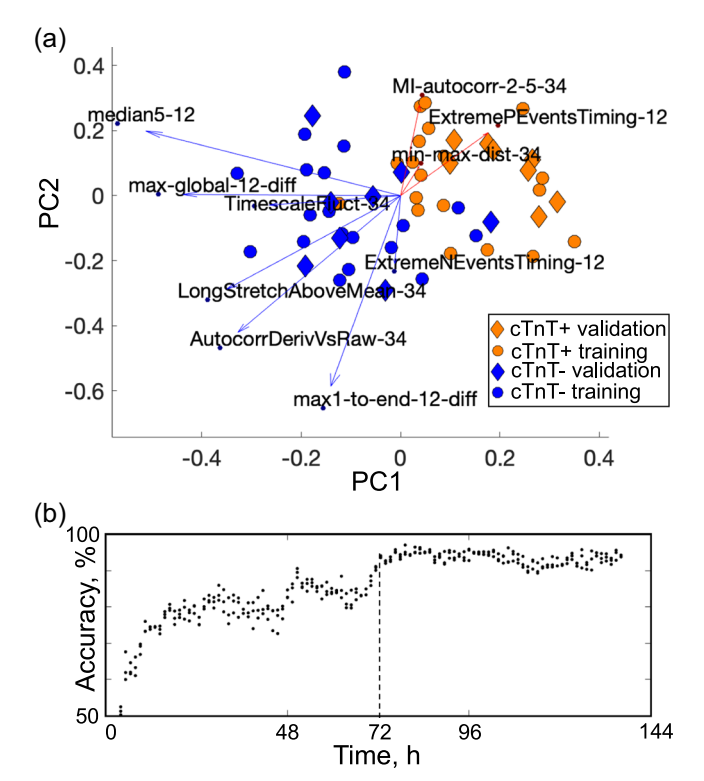


FIGURE 4 Partial least-squares discriminant analysis (PLS-DA) reveals clear separation of cTnT+ (cTnT > 30%) and cTnT- classes. (a) PLS-DA biplot shows projections of cTnT positive time series in orange and cTnT negative time series in blue. Loading vectors are colored according to their regression coefficient value, with positive regression coefficients colored red and negative colored blue. Only metrics from the first 72 h were used to yield validation accuracy of 94%. (b) Accuracy versus time passed after the initiation of the protocol. After the data from the first 72 h only is included in the analysis, the validation accuracy stops increasing with additional time series data included in the analysis.

excessive cell death (Figure S2) or a dramatic change in OCR timeseries shape or model performance (Figure S3).

In summary, the results presented in this communication reveal the first oxygen consumption-based method for prognostic prediction of the purity of a CM differentiation within the first few days of the protocol. Differences in the quality of starting material (e.g., heterogeneity of pluripotency, seeding density post-thaw) can impact the metabolic trajectories in the time window examined in this study. Notably, bioreactor conditions are distinctly different from multi-well culture plates-shear stress from mixing, growing in suspension instead of a monolayer and different spatial distribution of metabolites may affect the dynamics of OCR. However, the suggested approach can be translated to the data acquired from the bioreactor and the model can be re-trained, given that the predictive power of the derived metrics is already proven in principle. The Wnt signaling modulation protocol used to differentiate CMs in this article drives iPSCs to commit to mesoderm in the first 48 hours of differentiation and to cardiac mesoderm in the first 72 hours accompanied by a significant drop in mitochondrial DNA copy number (Mostafavi et al., 2021). Our results highlight the metabolic shift occurring in critical time window of the first 72 hours of the CM differentiation. Translation of our findings to cell manufacturing will greatly reduce costs of CM production by making the process more predictable, bringing iPSC-derived products one step closer to routine clinical use.

# 3 | MATERIALS AND METHODS

#### 3.1 | CM differentiation

Wells of a 96-well plate were coated with 100 µL Matrigel (GFR in Knockout D-MEM, 1:100, Thermo Fisher Scientific) per well and incubated for 1 h. HiPSC WTC11 cells were lifted from the maintenance plate with Accutase (Stemcell Technologies), mixed with DPBS (Thermo Fisher Scientific) at 1:3 ratio, centrifuged at 1000 rpm for 5 min, the supernatant was removed, and the pellet was lifted in media (basal MTeSR Plus media + supplement, 4:1, Stemcell Technologies) with Rock inhibitor (1000:1, Stemcell Technologies). A total of  $2 \times 10^4$  cells were seeded in 100 µL media with Rock inhibitor (1000:1) per well (day -2). Cells were fed MTeSR+ media on day -1 to reach 70%-90% confluency by day 0. On day 0 media is changed to RPMI plus B-27 Supplement minus insulin with 7.5 µM CHIR99021 (Stemcell Technologies). Exactly 48 h after (day 2), media is changed to RPMI plus B-27 Supplement minus insulin with 7.5 µM IWP2 (Stemcell Technologies). Another 48 h after (day 4), the media is changed to fresh RPMI plus B-27 Supplement minus insulin without any inhibitors. Next, cells are fed every 48 h with RPMI plus B-27 Supplement (with insulin). On day 16 cells are fixed and stained with cardiac troponin T (cTnT) monoclonal antibody (Thermo Fisher Scientific, clone 13-11). Wells were washed with 100 µL of phosphate-buffered saline (PBS) each (wash step) and then fixed with 100 µL of 4% paraformaldehyde solution in PBS for 10 min. After three wash steps, cells were permeabilized for 15 min with

 $100\,\mu L$  of 0.3% Triton X-100 solution in PBS. After a wash step, cells were blocked with  $100\,\mu L$  of Odyssey Blocking Buffer for 1 h at room temperature. Next, we diluted mouse anti-human cTnT primary antibody at 1:200 ratio in Odyssey Blocking Buffer and added to the cells for 1 h. Next, after three wash steps, cells were treated with  $100\,\mu L$  of Odyssey Blocking Buffer with anti-mouse Alexa Fluor Plus 488 secondary antibody (1:1000) for 30 min in the dark. Finally, after three wash steps  $100\,\mu L$  of PBS was added to each well and cells were imaged.

# 3.2 | Quantification of cardiac troponin T signal

Images of the stained wells were acquired with Nikon UltraVIEW VoX W1 Spinning Disk Confocal at  $\times 4$  magnification, and the entire well was captured with 4 FOVs stitched in a  $2\times 2$  grid. The resulting ".nd2" files were read using the Python nd2 library and the cTnT channel was extracted for thresholding. *OpenCV* library was used to blur the image with a  $75\times 75$  Gaussian kernel and extract cTnT positive pixels by Otsu's thresholding. Finally, the binary thresholded image was closed with a  $75\times 75$  circular kernel. Well diameter was manually measured using a corresponding brightfield image opened in ImageJ and the same value was used for all the images, assuming all the wells of the 96-well plate are of the same size. To calculate the % of cTnT signal in the well the sum of positive pixels in the thresholded image was divided by the measured well area in pixels.

#### 3.3 OCR time series metrics calculation

Real-time oxygen consumption measurement was done with a RESIPHER device (Lucid Scientific) with a 32-sensor lid compatible with a 96-well plate. Optical oxygen sensors are located at rows 3, 4, 9, and 10 of a 96-well plate. Data were sampled at a rate of 1 measurement in 15 min, comprising 96 timepoints per day. First, the time series were split into 3 regions: the first 48 hours after CHIR treatment (days 0 and 1), the next 48 h (days 2 and 3), and another 48 hours (days 4 and 5). The beginning of each region was equally cropped to exclude sharp fluctuations of flux that were occurring due to probe removal during media changes. Since previous studies showed that steady state of an open-air system with a monolayer of cells on the bottom of the well is reached within 1 hour of the media change, (Mamchaoui & Saumon, 2000) 4 timepoints were removed after every feed. After cropping, the total number of timepoints per the 48-hour time stretch comprised 176 points, with a total of 528 timepoints per experiment. Next, each of the regions was smoothed by the moving average with a window of 30 timepoints. Subsequently, for each region 8 median oxygen consumption levels were calculated for 8 consecutive nonoverlapping time windows of 22 points each. Finally, another 21 metrics were calculated for each region:

- plateau—the longest continuous time stretch where the values do not deviate from the mean of the stretch more than by 5% of the standard deviation of the total region
- max1 and argmax1—value and the time point of the first local maximum reached by the curve
- max2 and argmax2—value and the time point of the second local maximum reached by the curve
- max-global and argmax-global—value and the time point of the global maximum of the curve
- min1 and argmin1—value and the time point of the first local minimum of the curve reached after the first local maximum of the curve (to exclude the starting points from the minima)
- min-global and argmin-global—value and the time point of the global minimum of the curve reached after the first local maximum of the curve (to exclude the starting points from the minima)
- max-min-dist = argmin1-argmax1
- max-max-dist = argmax2-argmax1
- max-max-gap = max1-max2
- min-max-dist = argmax2-argmin1
- max-min-gap = max1-min1
- global-max-min-gap = max-global-min-global
- max1-to-end—time from the first local maximum (argmax1) to the end of the region
- max2-to-end—time from the second local maximum (argmax2) to the end of the region
- min1-to-end—time from the first local minimum (argmin1) to the end of the region
- length(num peaks)—total number of local maxima in the region

Overall, a total of 29 metrics were derived from each time series region. Next, the same 29 metrics were calculated for the derivative of each region, and the label "-diff" was added to the end of each corresponding metric name. To differentiate between the metrics derived from the different time regions the following naming rules were applied: label "12" in a variable name indicates that the metric was derived from the first 48 hours of the differentiation protocol, label "34" means the metric was derived from the next 48 hours, and label "56" means the metric was derived from the last 48 hours of the 6-day measurement process.

Additionally, 22 canonical time-series characteristics (catch22) defined in another study (Lubba et al., 2019) were included in the feature set. Features retained in the final models are listed in Table 1.

# 3.4 | Cell count tracking

We used mEGFP-tagged LMNB1 WTC iPS cell line purchased from Allen Institute (catalog number AICS-0013) to noninvasively monitor changes in cell count during the CM differentiation. First, we built a calibration curve to convert the GFP fluorescence intensity into cell count. We seeded iPSCs at a range of seeding densities  $(1-8.5\times10^4$  cells with a step of  $0.5\times10^4$  cells) in a 96-well plate and used a microplate reader (BioTek Synergy H1, Agilent Technologies) to register corresponding GFP intensities in the wells with the different cell counts. This resulted in a linear calibration curve. During CM differentiation experiments, the 96-well plate with iPSCs was unplugged from the RESIPHER device and transferred to the plate reader every 24 hours. Registered fluorescence intensities were converted to cell counts and were used to normalize the corresponding time window to obtain OCR values per cell.

# 3.5 | Multivariate regression

To assign a class label based on the % cTnT signal we performed Otsu's thresholding on a 1-d array of all % cTnT signal values. The X-block was structured from 58 curve metrics with additional 22 canonical time-series characteristics for each of the 3 time-series regions. In total, X-block comprised  $(58+22)\times 3=240$  features. We used a custom MATLAB script for both PLS regression and discriminant analysis. Y-block for regression was defined by % cTnT signal determined in section 5.2.2, for discriminant analysis Y-block was defined by % cTnT signal class label: cTnT+ or cTnT-. All features were normalized by standard deviation and centered by mean.

We used a 70:30 ratio of training to validation samples for cross-validation. During every iteration of cross-validation, samples were drawn at random from the cTnT+ class pool, and then a matching number was randomly drawn from the cTnT- pool. Due to the prevalence of cTnT- class, a random set of cTnT- samples was left out

**TABLE 1** List of canonical time-series characteristics retained after variable trimming in multivariate analyses.

HistogramMode-10	DN_HistogramMode_10	Mode of z-scored distribution (10-bin histogram).
MI-autocorr-2-5	CO_HistogramAMI_even_2_5	Automutual information, time shift 2, 5-bin histogram.
ExtremePEventsTiming	DN_OutlierInclude_p_001_mdrmd	Time intervals between successive extreme events above the mean.
ExtremeNEventsTiming	DN_OutlierInclude_n_001_mdrmd	Time intervals between successive extreme events below the mean.
AutocorrDerivVsRaw	FC_LocalSimple_mean1_tauresrat	Change in correlation length after iterative differencing
LongStretch AboveMean	SB_BinaryStats_mean_longstretch1	Longest period of consecutive values above the mean
TimescaleFluct	SC_FluctAnal_2_rsrangefit_50_1_logi_prop_r1	Proportion of slower timescale fluctuations that scale with linearly rescaled range

from the analysis on every iteration. To select the best predictors, we used variable trimming: iteratively removing every variable that reduced prediction accuracy averaged for 100 iterations of cross-validation.

#### **ACKNOWLEDGMENTS**

This material is based upon work supported by the National Science Foundation under Grant No. EEC-1648035. The authors gratefully acknowledge Dr. Walker Inman (Lucid Scientific) for helpful discussions.

#### DATA AVAILABILITY STATEMENT

The data that support the findings of this study are openly available in Github at https://github.com/kemplab/timeseries.

#### ORCID

Melissa L. Kemp http://orcid.org/0000-0003-3781-8802

#### REFERENCES

- van Berlo, J. H., & Molkentin, J. D. (2014). An emerging consensus on cardiac regeneration,". *Nature Medicine*, 20, 1386–1393.
- Floy, M. E., Shabnam, F., Simmons, A. D., Bhute, V. J., Jin, G., Friedrich, W. A., Steinberg, A. B., & Palecek, S. P. (2022). Advances in manufacturing cardiomyocytes from human pluripotent stem cells. *Annual Review of Chemical and Biomolecular Engineering*, 13, 255–278.
- Guan, X., Xu, W., Zhang, H., Wang, Q., Yu, J., Zhang, R., Chen, Y., Xia, Y., Wang, J., & Wang, D. (2020). Transplantation of human induced pluripotent stem cell-derived cardiomyocytes improves myocardial function and reverses ventricular remodeling in infarcted rat hearts. Stem Cell Research & Therapy, 11, 73.
- Lian, X., Hsiao, C., Wilson, G., Zhu, K., Hazeltine, L. B., Azarin, S. M., Raval, K. K., Zhang, J., Kamp, T. J., & Palecek, S. P. (2012). Robust cardiomyocyte differentiation from human pluripotent stem cells via temporal modulation of canonical Wnt signaling. *Proceedings of the National Academy of Sciences*, 109(27), E1848–E1857.
- Lubba, C. H., Sethi, S. S., Knaute, P., Schultz, S. R., Fulcher, B. D., & Jones, N. S. (2019). catch22: CAnonical Time-series CHaracteristics. *Data Mining and Knowledge Discovery*, 33, 1821–1852.
- Mamchaoui, K., & Saumon, G. (2000). A method for measuring the oxygen consumption of intact cell monolayers. American Journal of Physiology-Lung Cellular and Molecular Physiology, 278(4), L858–L863.
- Manstein, F., Ullmann, K., Kropp, C., Halloin, C., Triebert, W., Franke, A., Farr, C.-M., Sahabian, A., Haase, A., Breitkreuz, Y., Peitz, M.,

- Brüstle, O., Kalies, S., Martin, U., Olmer, R., & Zweigerdt, R. (2021). High density bioprocessing of human pluripotent stem cells by metabolic control and in silico modeling. *Stem Cells Translational Medicine*, 10(7), 1063–1080.
- Mostafavi, S., Balafkan, N., Pettersen, I. K. N., Nido, G. S., Siller, R., Tzoulis, C., Sullivan, G. J., & Bindoff, L. A. (2021). Distinct mitochondrial remodeling during mesoderm differentiation in a human-based stem cell model. Frontiers in Cell and Developmental Biology, 9, 744777.
- Qian, T., Heaster, T. M., Houghtaling, A. R., Sun, K., Samimi, K., & Skala, M. C. (2021). Label-free imaging for quality control of cardiomyocyte differentiation. *Nature Communications*, 12, 4580.
- Shiba, Y., Gomibuchi, T., Seto, T., Wada, Y., Ichimura, H., Tanaka, Y., Ogasawara, T., Okada, K., Shiba, N., Sakamoto, K., Ido, D., Shiina, T., Ohkura, M., Nakai, J., Uno, N., Kazuki, Y., Oshimura, M., Minami, I., & Ikeda, U. (2016). Allogeneic transplantation of iPS cell-derived cardiomyocytes regenerates primate hearts. *Nature*, 538, 388-391.
- Vormittag, P., Gunn, R., Ghorashian, S., & Veraitch, F. S. (2018). A guide to manufacturing CAR T cell therapies. Current Opinion in Biotechnology, 53, 164–181.
- Williams, B., Löbel, W., Finklea, F., Halloin, C., Ritzenhoff, K., Manstein, F., Mohammadi, S., Hashemi, M., Zweigerdt, R., Lipke, E., & Cremaschi, S. (2020). Prediction of human induced pluripotent stem cell cardiac differentiation outcome by multifactorial process modeling. Frontiers in Bioengineering and Biotechnology, 8, 851.
- World Health Organization (WHO), "Cardiovascular diseases (CVDs)," 11 June 2021. [Online]. Available: https://www.who.int/en/news-room/fact-sheets/detail/cardiovascular-diseases-(cvds)

### SUPPORTING INFORMATION

Additional supporting information can be found online in the Supporting Information section at the end of this article.

How to cite this article: Nikitina, A. A., Roysam, T., & Kemp, M. L. (2023). Early dynamic changes in iPSC oxygen consumption rate predict future cardiomyocyte differentiation. *Biotechnology and Bioengineering*, 120, 2357–2362.

https://doi.org/10.1002/bit.28489